Received XX Month, XXXX; revised XX Month, XXXX; accepted XX Month, XXXX; Date of publication XX Month, XXXX; date of current version XX Month, XXXX.

Digital Object Identifier 10.1109/XXXX.2022.1234567

Field Deployment of BiodivX Drones in the Amazon Rainforest for Biodiversity Monitoring

Christian Geckeler[1,2], Steffen Kirchgeorg[1,2], Georg Strunck[3], Frederik Bendix Thostrup[4], Florencia Sangermano[5], Andrea Desiderato[6], Martina Lüthi[7], Meret Jucker[7], Mailyn Adriana Gonzalez Herrera[8], Nicolás D. Franco-Sierra[9], Paola Pulido-Santacruz[10], Jia Jin Marc Chang[11,12], Yin Cheong Aden Ip[13], Elvira Mächler[14], Asger Svenning[15], Guillaume Mougeot[15] Toke Høye[15], Fabian Fopp[7,2], Loic Pellissier[7,2], David Dao[16], Kristy Deiner[14,17], Claus Melvad[4], Salua Hamaza[3], and Stefano Mintchev[1,2]

[1]Environmental Robotics Laboratory, Dep. of Environmental Systems Science, ETH Zurich, 8092 Zurich, Switzerland
[2]Swiss Federal Institute for Forest, Snow and Landscape Research (WSL), 8903 Birmensdorf, Switzerland
[3]Biomorphic Intelligence Lab, Faculty of Aerospace Engineering, TU Delft, 2629HS Delft, The Netherlands
[4]Department of Mechanical and Production Engineering, Aarhus University, Aarhus, Denmark
[5]Graduate School of Geography, Clark University, 950 Main Street, Worcester, MA, 01610, USA
[6]Department of Invertebrate Zoology and Hydrobiology, Faculty of Biology and Environmental Protection, University of Lodz, Lodz 90-136, Poland
[7]Ecosystems and Landscape Evolution, ETH Zürch, Zürich 8092, Switzerland
[8]Alexander von Humboldt Biological Resources Research Institute, Bogotá 111311, Colombia
[9]Syndesis Health, Palm Beach Gardens, Florida 33408, United States
[10]Department of Biology, Faculty of Natural Sciences, Universidad del Rosario, Bogotá 111221, Colombia
[11]Department of Biological Sciences, National University of Singapore, Singapore 117558, Singapore
[12]Lee Kong Chian Natural History Museum, National University of Singapore, Singapore 117377, Singapore
[13]School of Marine and Environmental Affairs, University of Washington, Seattle, Washington 98105, United States
[14]SimplexDNA AG, Winterthur 8404, Switzerland
[15]Department of Ecoscience, Aarhus University, C.F. Møllers Allé 8, 8000 Aarhus C, Denmark
[16]GainForest,Schwandenacker 35, 8052 Zurich, Switzerland
[17]Environmental DNA, ETH Zürich, Zürich 8092, Switzerland

Corresponding author: Christian Geckeler (email: cgeckeler@ethz.ch).

This work was supported by the Swiss National Science Foundation through the Eccellenza grant (grant number 186865). It was further supported by the Rütli-Stiftung, the ETH Foundation, the XPRIZE Foundation, and the Alana Foundation via the participation of the authors in the XPRIZE Rainforest competition. Salua Hamaza's work was supported by NWO VENI grant 20308.

ABSTRACT Tropical rainforests are among the most biodiverse ecosystems on Earth, and also among the most threatened by anthropogenic pressures such as deforestation and climate change. Understanding human impact and the efficacy of conservation and preservation efforts requires scalable and comprehensive biodiversity monitoring solutions. As a winning finalist of the XPRIZE Rainforest Competition, ETH BiodivX collected biodiversity data from 100 ha of rainforest in the Amazon, in 24 hours. A suite of complementary data types were captured, from remote sensing maps and close-up images to surface and water environmental DNA (eDNA), along with canopy rafts which collect specimens, close-up images, and bioacoustic recordings. A distributed mesh communication network allows for a persistent link to the drone, up to the edges of the competition area. Optimized workflows allow for a full RGB and digital surface map (DSM) after only one-and-a-half hours. The captured DSM was then used to collect surface eDNA fully autonomously, and using the communication network, surface eDNA was collected at distances up to 1.4 km from the base station. Pre-processed multispectral satellite remote sensing provides indicators of water locations, which were then sampled for water eDNA. The canopy rafts can act as communication nodes or data collection stations, providing long-term bioacoustic recordings, insect images, and specimens. By utilizing a commercial drone platform with modular payloads for diverse tasks, the solutions are robust and easy to use. These field-proven systems mark a major step towards scalable biodiversity monitoring, including in some of the world's most remote and biodiverse regions: tropical rainforests.

INDEX TERMS biodiversity assessments, environmental monitoring, drones, canopy raft, environmental DNA, remote sensing, insect trap

I. INTRODUCTION

TROPICAL rainforests are among the most biodiverse ecosystems on Earth, home to a large diversity of species of plants, animals, fungi, and microorganisms, many of which remain undiscovered. This biodiversity is vital to maintain ecosystem functions, such as carbon sequestration, water cycling, and oxygen production, which, in turn, are essential for regulating the global climate and supporting life on Earth [1], [2].

Despite the global significance of rainforests, the composition and distribution of their biodiversity remains unexplored and poorly documented [2]. Rainforest ecosystems harbor over half of the world's terrestrial vertebrate species, but many areas have not been studied, and large information gaps exist [3]. Even as new species are regularly discovered, there is still limited knowledge about their role within the ecosystem, their interactions with other species, and their response to environmental changes. This lack of information is concerning given the accelerating threats of deforestation and climate change, which may drive species to extinction before they can be studied and their role understood. Undiscovered species are often the most endangered ones, underpinning the necessity for more thorough research of rainforests [4], [5]. Anthropogenic pressures from deforestation, habitat fragmentation, and climate change endanger not only the local species but also the ecosystem's overall health and functioning [6]. Therefore, research to understand the impacts of human activities on these ecosystems and to develop effective conservation strategies is urgently needed. Studying rainforest biodiversity aids in understanding the intricate relationships between species and their environment, guiding ecosystem management and restoration efforts, and lay the foundation for sustainable land use.

Our understanding of rainforests and the diverse life thriving within their canopies depends on our ability to collect samples, conduct observations, and gather data at meaningful ecological scales [7]. However, accessing the various layers of forests, from the ground to the highest emergent trees, remains costly, risky, and difficult to achieve with adequate spatial and temporal resolution [8], [9]. To overcome these limitations, the XPRIZE Rainforest competition was launched in 2019 to catalyze the development of technologies capable of surveying biodiversity across all layers of vast rainforest areas within constrained timeframes [10]. The competition aims to empower ecosystem stewardship and conservation efforts by providing critical data at scale to inform action and policy, support sustainable bioeconomies, and amplify the role of Indigenous Peoples and local communities (IPLCs), who serve as the primary protectors and knowledge holders of the planet's tropical rainforests.

This paper outlines the robotics methodologies and technologies underpinning the integrated biodiversity survey approach developed and deployed by the ETH BiodivX team during the XPRIZE Rainforest competition finals in the Amazon rainforest. For our efforts, our team was awarded the XPRIZE Rainforest Bonus Prize of USD $250 000.

First, in Section II, we provide an overview of the state of the art, focusing specifically on robotic systems designed for operation in forest and canopy ecosystems. In Section III we give an overview of the competition and requirements for the solutions, as well as the judging criteria, which motivated several design choices. Next, in Section IV we give a high-level overview of the different components of our robotic strategy. In Section V and Section VI we describe the satellite and drone remote sensing, and in Section VII the communication components of our solution. Then, we describe our data collection solutions, starting with environmental DNA (eDNA) in Section VIII and water eDNA in Section IX. Section X describes the structure of the canopy rafts, their deployment and collection strategies, as well as their payloads for collecting multiple data types. We showcase some results in Section XI, discuss them in Section XII, and conclude the paper in Section XIII.

II. STATE OF THE ART

Forest canopies are the last ecological frontier, characterized by a structural complexity that creates unique habitats and microclimatic conditions for life to thrive [8], [11]. Developing scalable and comprehensive methods to monitor this biodiversity is both urgent and an open scientific and technological challenge [12]. Traditional approaches such as visual surveys, traps, and fumigation are labor-intensive, spatially and temporally constrained, require taxonomic expertise, and can be invasive to the target ecosystem or species [13], [14]. In tropical forests, a large fraction of the species occupy tree canopies, and accessing this habitat represents further challenges. Traditional and modern survey tools, including camera traps, bioacoustic sensors, and eDNA surveys, face limitations due to the inherent difficulties of accessing tree canopies, which restrict in-situ observations, manual sampling, and sensor deployment capabilities. Methods such as rope climbing [15], [16], crane use [17], manned aerial platforms like blimps, and walkable canopy rafts [18] have been employed to gain access to tree canopies. However, these approaches are often costly, logistically demanding, and lack the spatial and temporal scalability needed for broad applications [9], [11].

Robots offer a promising solution to address the challenge of accessibility [9]. Among these, drone-based approaches have recently gained prominence as transformative tools for exploring and gathering data in forest environments. These technologies enable a range of innovative biodiversity survey solutions, including aerial remote sensing [19], [20], sound recordings via microphone payloads [21], insect specimen collection by dragging nets [22], sampling of twigs form outermost canopy layers [23], [24], sensor placement on branches [25]–[29], and eDNA sampling [30], [31]. It is this type of robot that we have selected for the competition.

III. COMPETITION OVERVIEW AND CHALLENGES

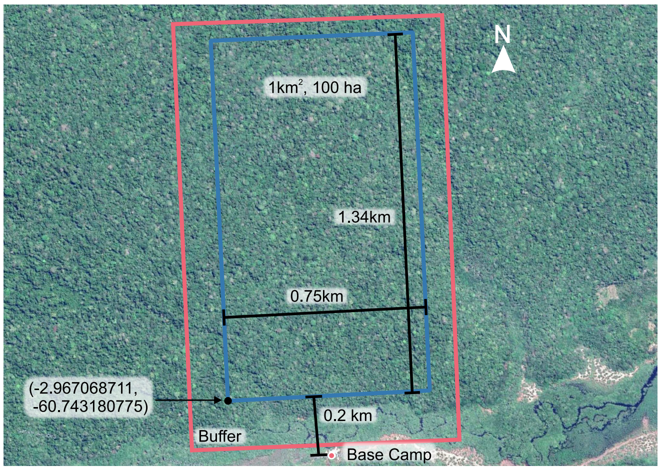

FIGURE 1. Overview of the competition area (blue), which is 0.75 km by 1.34 km. The total area is 1 square kilometer or 100 ha. The distance from the base camp to the border is at least 200 m. Entry into the red buffer zone is forbidden. Map underlay from Google Maps 2025, Airbus, CNES, Maxar Technologies.

The main goal of the XPRIZE Rainforest competition is to generate the most comprehensive insights into the biodiversity of 100 ha of rainforest within a limited time frame. The geographical location of the competition plot is disclosed to the teams 24 hours before the start of the data collection phase. The competition area can be seen in Figure 1, it is 1.34 km long by 0.75 km wide, and it is located in the Brazilian Amazon Rainforest (bottom left corner is at -2.967068711 latitude, -60.743180775 longitude). Each team is allocated 24 hours, commencing at 12:00, to collect biodiversity data, adhering to the strict requirement that all data must be collected remotely. Team members are confined to a designated base camp, separated from the competition area by a buffer zone of at least 0.2 km. The prohibition of human entry into survey sites restricts feasible methods to remote sensing and robotic technologies capable of transporting and deploying sensors. Following the data collection phase, teams are granted an additional 48 hours to analyze the data and derive meaningful insights. These may include, for example, the discovery of new ecological relationships or dependencies between biodiversity and climate, identification of ecosystem threats and potential solutions, anthropological insights, integration of Indigenous knowledge, sustainable human–rainforest interactions, educational opportunities, or pathways toward effective conservation actions and policies at local, regional, and international levels.

A panel of independent judges evaluated each team's performance based on a combination of qualitative and quantitative criteria. Table Table 1. summarizes the most influential criteria that guided the design of our biodiversity survey strategy and shaped the development of our robotic systems.

The qualitative assessment focuses on a scoring system that measures each team's ability to detect the highest number of plant and animal species, referred to as observed species richness. Tropical rainforests exhibit the highest species-to-area relationship of any terrestrial ecosystem [32], largely due to their complex, vertically stratified canopy structure. Many species occur only within specific tree hosts and forest layers, such as vascular epiphytes, insects, or birds. To achieve a comprehensive species inventory, it is important to deploy an integrated survey strategy based on multiple data types, such as images, sounds, and eDNA. Moreover, survey methodologies must enable rapid surface coverage (e.g., through remote sensing imaging) and vertical penetration from the canopy to the forest floor (e.g., with sensors capable of vertically surveying through the forest strata). Alternatively, techniques that integrate data from spatially dispersed sources, such as acoustic sensors [33], light traps [34], or environmental DNA collected from flowing water [35], provide complementary approaches.

Four qualitative criteria had a direct impact on the design of our robotic platforms. One of the main requirements was system autonomy. Autonomous or semi-autonomous solutions were preferred over fully remote-controlled systems, as dense vegetation severely limits communication range and makes continuous teleoperation unreliable. To address this, we focused on automating navigation, data acquisition, and sample collection whenever possible. In addition, we deployed mesh communication networks to extend coverage of a backup communication network, for monitoring, supervision, and the transmission of high-level commands to ensure operational safety.

Another key requirement was to minimize the risk of equipment loss. The structural complexity of rainforest vegetation makes ground robots and aerial vehicles operating below the canopy particularly vulnerable to entanglement, collisions, and crashes. As a result, we performed aerial operations above the canopy, where visibility and freedom to maneuver are greater. To enable sampling through the forest strata, we equipped the aerial platforms with end-effectors capable of reaching the forest floor and penetrating canopy layers.

Technology readiness was also an important evaluation criterion. The judges required systems to be at least at technology readiness level (TRL) 7, meaning they should

Category	Criteria	System Components
1. Biodiversity Surveying	Remote survey of 100 ha of tropical rainforest within 24 hours	Diverse Data: eDNA, remote sensing, bioacoustics, and physical samples
2. Scalability, Performance, and Autonomy	Demonstrate ability to scale technology to larger regions (minimum TRL 7)	Both remote controlled and fully autonomous operations
3. Innovation and Technological Advancement	Developing novel, disruptive technologies	Incorporation of robotics, AI, remote sensing, and in-field DNA analysis
4. Real-Time Insights	Generate impactful insights within 48 hours of analysis	Species richness, detect ecological dependencies, identification of threats, potential economic opportunities
5. Community Collaboration	Incorporate Indigenous and local community (IPLC) knowledge and participation	Co-design and scale solutions with IPLC team members

TABLE 1. Requirements, judging criteria and system components. Categories 1-3 are described in this manuscript.

be robust, field-tested, and easy to operate in challenging rainforest conditions. To meet this requirement, we built upon commercially available drone platforms and concentrated development efforts on modular end-effectors and sensor payloads.

Portability and ease of deployment were additional quantitative evaluation criteria. Systems that could be carried by hand and quickly deployed in the field received higher scores. To address this, we reduced the types of robotic platforms used in our approach to one primary drone platform, which allowed us to increase redundancy in critical components such as batteries and controllers and simplify field logistics.

IV. SYSTEM OVERVIEW

We developed a drone-based survey methodology to address the requirements and challenges outlined in the previous section. Figure 2 provides a graphical summary of this solution, which employs aerial robots to collect diverse data streams from all forest layers. The key components of this methodology include:

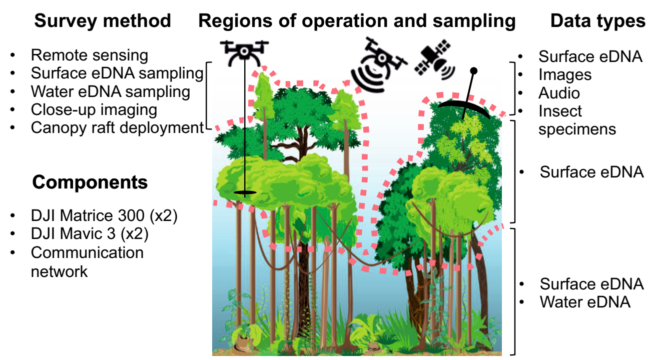

	Teleoperation	Autonomy Level 1	Autonomy Level 2
Flight control	Autonomous flight stabilization and obstacle avoidance	Autonomous flight stabilization and obstacle avoidance	Autonomous flight stabilization and obstacle avoidance
Flight path	Pilot is in control	Pilot is in control	Autonomous
Sampling	Pilot is in control	Autonomous	Autonomous
Communication	Connectivity with remote controller required	Connectivity with remote controller required	Optional for supervision
	• **Raft deployment** • **Close-up canopy (with Mavic 3)**	• **Water eDNA sampling** • **Surface eDNA sampling**	• **Surface eDNA sampling** • **Remote sensing** • **Close-up imaging (with M300)**

Short → Long
Range of deployment

FIGURE 2. Overview of the system, detailing the above-canopy survey methods, main components, types of data collected across different forest strata, and the level of autonomy achieved.

- **Remote Sensing:** Satellite- and drone-based imaging of the 100-hectare competition area for photogrammetry and mapping (see Section V and VI).
- **Surface eDNA Sampling:** Collection of eDNA from various canopy layers using a specialized probe lowered into the canopy from a DJI M300 drone (see Section VIII).
- **Water eDNA Sampling:** Collection of eDNA from accessible water bodies using a water pump system lowered from a DJI M300 drone (see Section IX).
- **Close-Up Imaging:** High-resolution images of the forest canopy, captured for plant identification and scouting regions of interest (e.g., water access, flat canopies suitable for raft deployment). These images were obtained using a DJI M300 drone equipped with a Zenmuse H20 camera and the DJI Mavic 3 Series drone (see Section VI).
- **Canopy Rafts:** Sensor nodes equipped with light traps, microphones, and adhesive traps for collecting insect specimens. These systems are deployable by drones onto the upper surfaces of tree canopies (see Section X).
- **Communication Network:** A long-range communication network comprising static and mobile mesh

nodes to ensure operational supervision over the entire competition area (see Section VII).

This solution enables the collection of four key types of data and samples—audio, imagery, specimens, and eDNA—across the entire competition area and from multiple forest layers (Figure 2). Our framework adopts a modular approach, employing swappable payloads for a single drone system to significantly reduce logistical overhead, such as managing batteries, transporting multiple drone types, and ensuring field readiness. These modules include a mechanism for deploying canopy rafts (Section X, either for communication, or collecting specimens, bioacoustic data and eDNA), a camera (Section VI, for either photogrammetry mapping or close-up pictures), or a winch payload (Section VIII and Section IX, with either a surface probe or water pump for surface and water eDNA, respectively). Drones are operated safely above the canopy to minimize collision risks. The sampling methods feature varying levels of autonomy, categorized into three levels based on the degree of autonomy required for flight path control and sampling operations. To further enhance safety, a mesh network was implemented to monitor and supervise some of the autonomous tasks. The primary workhorses for these tasks were two DJI M300 drones, which could perform most sampling tasks through simple payload swaps. The drone fleet also included a DJI Mavic 3 Pro and a DJI Mavic 3 Classic, used primarily for close-up imaging, scouting, videography, and providing reference viewpoints (e.g., for canopy raft deployment). The simultaneous use of multiple drones was essential for parallelizing workflows, maximizing data collection within the 24-hour sampling timeframe imposed by the competition, and providing redundancy to enhance safety in case of failures. In the following sections, each sampling solution is described in detail.

V. SATELLITE REMOTE SENSING

High resolution (50 cm) multispectral satellite imagery from Planet SkySat Analysis-ready, and medium resolution (30 m) Landsat imagery, were used to assess the general characteristics of the area before the start of the 24 hours sampling. Analysis of remotely sensed images allowed identifying potential presence of water for eDNA sampling, assess spectral diversity, which is known to be related to functional and structural properties of the canopy cover and its diversity [36], identify areas of potential secondary forest, and the determination of regions of interest. These regions were selected based on factors such as proximity to water and vegetation heterogeneity, which guided the deployment of canopy rafts.

The Planet image was acquired on April 14, 2024 and consists of four bands measuring surface reflectance in the blue (450-515 nm), green (515-595 nm), red (605-695 nm), and near-infrared (740-900 nm) parts of the electromagnetic spectrum. The analysis-ready images were orthorectified and calibrated to surface reflectance, without requiring further pre-processing.

Traditional true and false color composites (Figure 3A and B) did not highlight the spatial heterogeneity of the region. Thus, a false color composite of indices was generated to highlight high reflective areas, including mostly white sand beaches and bright tree leaves, vegetation productivity, and moisture content (Figure 3C). The high reflective areas index was calculated through a color transformation of the RGB bands into a HIS (hue, illumination, saturation) space. The index was generated as: $\frac{Illumination-saturation}{Illumination+saturation}$. The Enhanced Vegetation Index (EVI) [37], was used as the component of vegetation productivity, as has been shown to be well correlated with leaf area index (LAI), biomass, canopy cover, and absorbed photosynthetically active radiation. Finally, water content was mapped using the McFeeters water index [38].

Spectral diversity is the variation of surface reflectance across space. The average coefficient of variation for a 10 m circular moving window was calculated for each band and then averaged across all bands [36]. A moving window of a radius of 10 m was chosen as it is the approximate crown size in the area, established by measuring a sample of trees, and matches the mean crown size of 10.6 m identified in Para, Brazil [39] . This allowed highlighting areas with higher spectral diversity than average (Figure 3D). Finally, a Landsat time series from 1985 to 2022 were analyzed with Google Earth Engine LandTrendr [40] to identify the year of the start of forest regrowth (Figure 3D).

The index color composite, together with the spectral diversity, and year of regrowth image, allowed a better visualization of forest heterogeneity, identifying potential water areas in the southwest and northeast of the testing area, as well as an area of potential forest regrowth to the southeast. Based on this information, we selected the southeast, south, and southwest regions of the testing area to scout for suitable locations for raft deployment.

VI. DRONE REMOTE SENSING

The drone remote sensing comprises two activities, mapping and close-up images. Mapping is done autonomously and processed into first a relatively low-resolution map which is useful for giving a situational overview and for tree canopy delineations, and then a higher resolution map which can provide more detailed information, especially regarding elevation. High-resolution close-up images are captured both autonomously across the entire competition area, and manually within teleoperation range for certain points of interest.

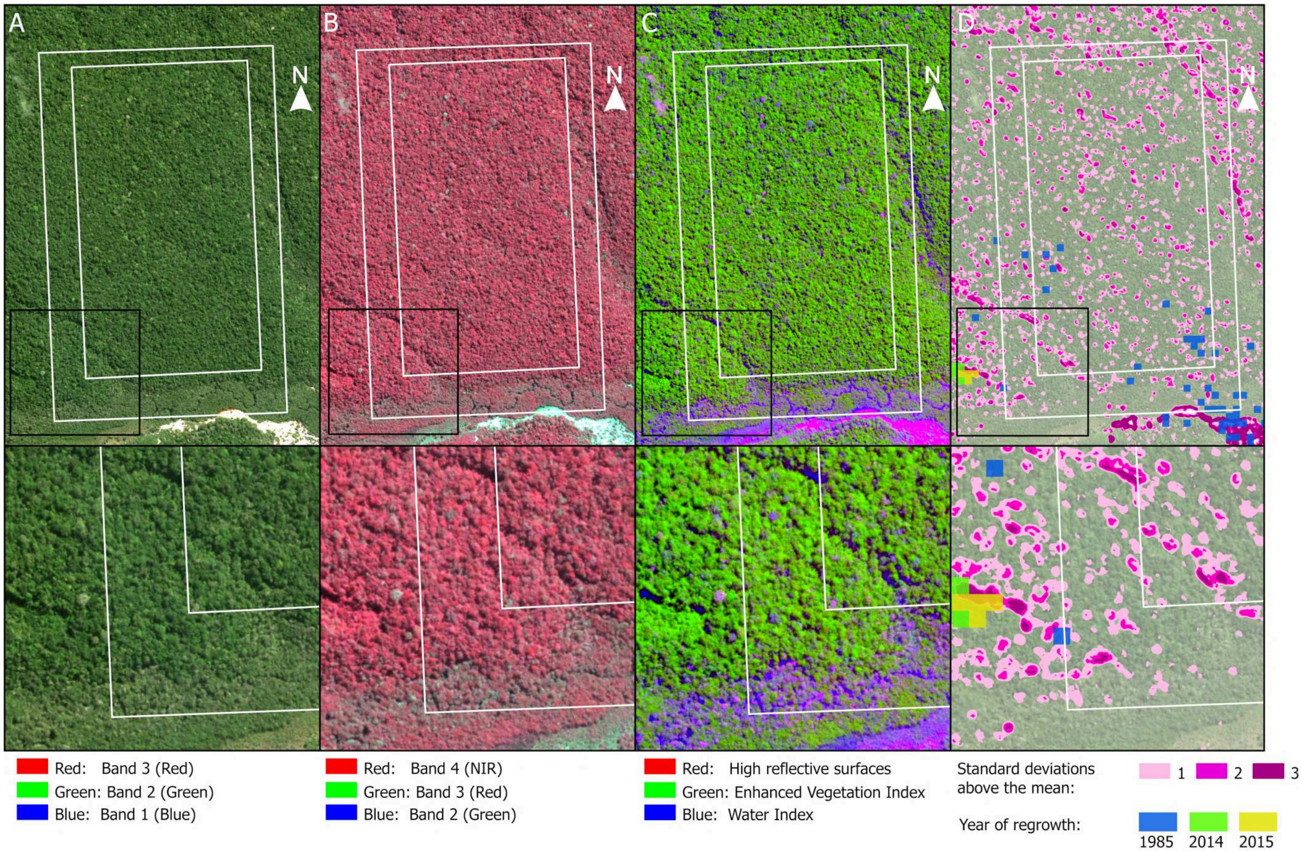

FIGURE 3. Inner white rectangle is the competition area, the outer white rectangle is the buffer zone. A) True color composite B) False color composite, C) Index composite, D) High spectral diversity areas and year of the start of forest regrowth.

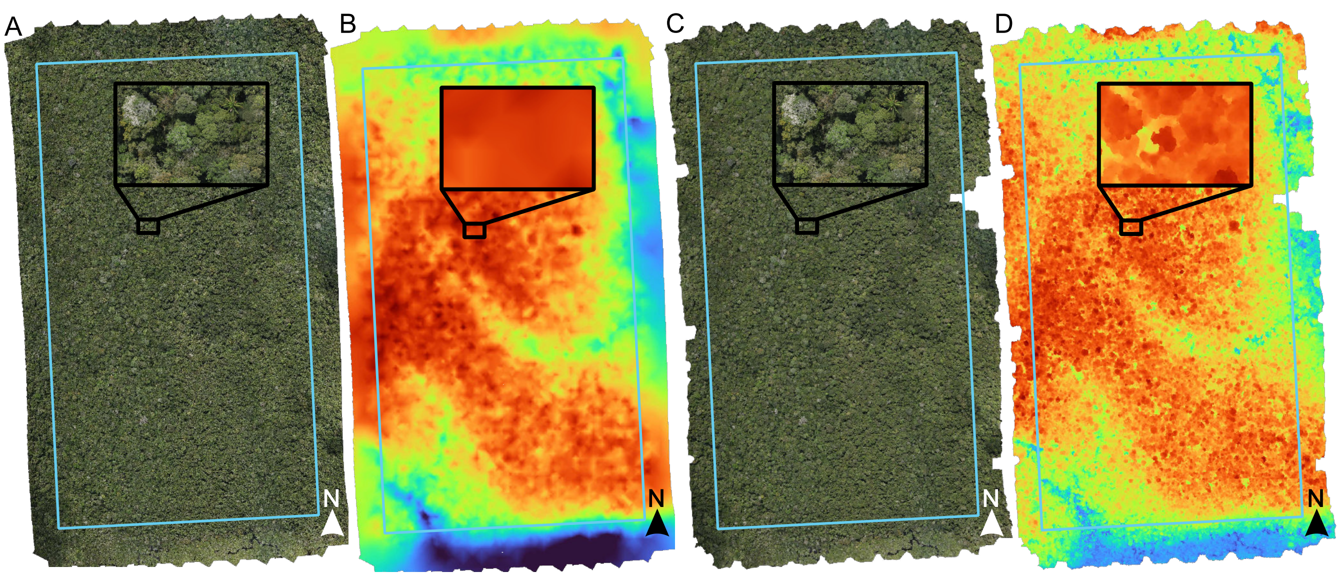

FIGURE 4. RGB Orthomosaics (A,C) and DSMs (B,D) generated with PIX4DReact (A,B), and PIX4DMatic (C,D). Insets show a zoomed-in view.

The first task of the competition was to create a map, both for its direct informational value, which served to identify plant species and generate ecological insights from the imagery, and as a necessary step to plan and conduct autonomous missions for surface eDNA sampling. To facilitate downstream tasks which require the RGB orthomosaic and digital surface model (DSM), an initial result, even with reduced quality, is essential. The RGB orthomosaic map can be directly further processed by algorithms for tree crown delineation and species identification, already providing initial quantitative results. The maps can also be directly used to inform further sampling, by detecting promising locations for surface eDNA sampling, or potential locations for water sampling. Autonomous surface eDNA sampling requires an up-to-date, high-resolution canopy height map, both for drone safety and sample probing depth, which the DSM provides. To this end, photographs of the entire 100 ha with the DJI Zenmuse P1, an RGB photogrammetry camera for the DJI M300, were captured. Then, the data was quickly processed to get a workable, albeit lower-resolution map for canopy height. After this, the processing is started for a higher resolution map which, while more detailed, is also more time- and processing-intensive. Using the initial map, the next sampling missions can already be planned while the higher resolution and more accurate map is processed. After this more accurate map is processed, the increased accuracy can be used for more challenging missions, such as flying closer to the treetop canopy or with reduced visibility, such as at night, where manual visual safety checks are more challenging. Since the exact coordinates of the 100 ha area were published 24 hours in advance, photogrammetry flights to cover the area were planned in advance. The default DJI flight planning software was used to plan the photogrammetry missions, while UgCS from SPH Engineering [41] was used to plan the rest of the flights. The photogrammetry missions had the following settings: 80% horizontal and vertical overlap and a flight altitude of 200 m. With the 35 mm lens on the DJI Zenmuse P1 and the chosen flight height, this results in a theoretical ground sample distance (GSD) of up to 1.56 cm/pixel. The altitude was chosen as a trade-off between time needed for data capture, time needed for processing, and the resulting resolution. Two mapping flights were needed to cover the entire area, which took 50 minutes and resulted in 1064 images.

The rapid initial processing into an orthomosaic and DSM was performed with PIX4DReact, a Structure from Motion (SfM) photogrammetry tool for first responders from PIX4D [42]. While the software offers less flexibility and less accurate output when compared with other options, the processing is extremely fast. For the roughly thousand captured images, processing only took half an hour with an average GSD of 2.52 cm/pixel (results can be seen in Figure 4A,B). Therefore, the full initial RGB orthomosaic and DSM of the 100 ha were available after one and a half hours, from data capture to completed processing.

After the initial PIX4DReact processing, a separate higher resolution but more computationally intensive reconstruction was performed, using PIX4Dmatic. Using the same hardware, this processing took almost five hours and can be seen in Figure 4C,D with a GSD of 2 cm/pixel.

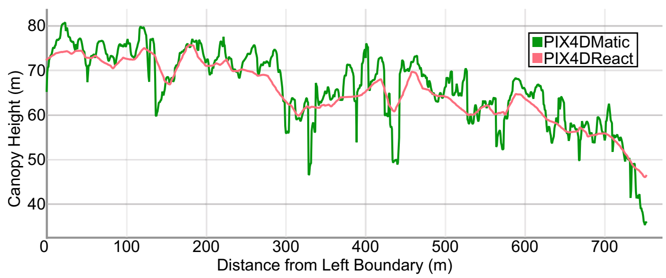

FIGURE 5. **Elevation profile of a sample horizontal transect for DSMs generated with PIX4DReact (red) and PIX4Dmatic (green), units are in m (distance from left-most competition boundary on the x-axis, canopy height on the y-axis).**

Qualitatively judging the visual differences between the orthomosaics can be difficult, however, the DSM exhibits significant differences, with deviations of up to dozens of meters (Figure 5). Figure 5 shows the height profile for a sample horizontal transect of the two DSMs and the corresponding differences. It is clear that while the DSM from PIX4DReact provides an initial estimate for the canopy height that is more accurate than available satellite data, more detailed height differences with trees emerging from the canopy or gaps between trees cannot be detected. For this, the more detailed DSM should be used. When planning missions with the PIX4DReact DSM, the values were used as an initial estimate, padding the waypoints with enlarged safety margins to compensate.

Close-up images were captured both autonomously and using teleoperation. Autonomous close-up images were captured across the entire competition area using the DJI M300 and DJI Zenmuse H20. The more than 20x optical zoom provides high resolution close-up images of tree canopies, while still allowing the drone to fly relatively high and cover a larger area. These images enable tree species identification, especially with the presence of distinctive features such as leaves or flowers (see Figure 12). Autonomous close-up images were captured across three vertical transacts spanning the entire competition area, see Figure 11. For additional data, and to utilize human experts for flora identification, manual close-up images were also captured using a DJI Mavic 3 Pro. Using manual flights within operation range, this

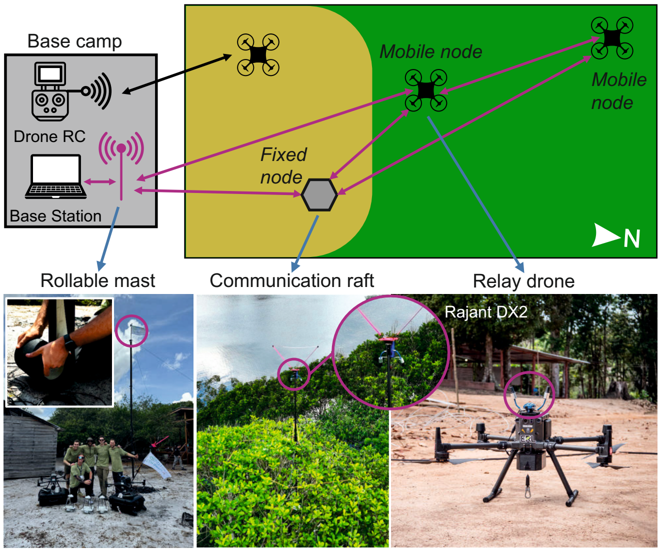

FIGURE 6. Overview of the communication system used, nodes of the 2.4GHz mesh network are circled. The southern third of the competition area (in tan) is within range of teleoperation of the remote controller, whereas for communication access to the rest of the competition area (in green), the fixed and mobile nodes of the mesh network are needed.

resulted in close-up images within the lower third of the competition area. This range is possible due to the relatively high altitude of the drone, which maintains the connection to the remote controller but can still deliver high resolution images with 7x optical zoom. In addition to flora identification, the DJI Mavic 3 Pro was also utilized to verify the location of water sampling sites identified through the satellite remote sensing and mapping, as well as provide an additional viewpoint during the raft deployment, enhancing safety.

VII. COMMUNICATION

One of the largest robotics challenges in surveying the 100 ha is communication. If the robots are teleoperated, a continuous communication link is needed to control and receive feedback from the robot. If the robot is fully autonomous, then it is also possible to move beyond the communication range of the ground station and pilot, under the assumption that safety mechanisms will ensure flight and operational safety under all eventualities. Indeed, for the mapping flights, the connection between the remote controller (RC) and drone was lost for the last third of the area, during this time the uncrewed aerial vehicle (UAV) was flying and capturing data fully autonomously, with no communication link. Since lowering a probe into the vegetation is more risky than capturing images from above, for surface eDNA sampling it was decided to utilize a back-up communication channel which would directly connect with the onboard computer, located in our custom payload, see Section VIII. This communication link from the base station to the communication node on the drone can provide feedback to the operator on the current sampling status as well as trigger or abort commands.

Looking at Figure 1, it is apparent that while the competition area is 100 ha, it is longer than it is wide. This means that under consideration of the minimum 200 m wide buffer zone, the distance from the pilot's position at the base camp to the furthest point within the competition area is around 1.4 km. Despite impressive ranges on the spec sheets, the actual range for both the stock DJI Antenna and similar communication devices is much less than advertised (up to 14 km under ideal conditions). In our field conditions, communication became unreliable after around 500 m from the base station at canopy height. This is mainly due to the environment, occlusions, and the drone position. Since the pilot's position is not elevated, trees between the pilot's position and the UAV reduces the range due to the Fresnel effect. Since the drone is less than 20 m from the canopy for surface eDNA sampling, this effect is even more prevalent than if it was flying at higher altitudes, such as during mapping for instance. Rainforests, with high humidity, dense foliage, and potentially also fog, present a particularly challenging environment for communication devices.

Therefore, a node-based 2.4 GHz mesh network (based on the Rajant Breadcrumb DX2 [43]) was chosen as an alternative communication link. The mesh network removes the need to reliably maintain a single monolithic connection, instead, multiple nodes can extend the range while also providing redundancy. 2.4 GHz provides ample data bandwidth and was shown during testing to also maintain sufficient range under the described conditions. The communication node on the drone is directly connected via LAN cable to the onboard computer, which then interfaces with the drone via the proprietary DJI Payload SDK. This permits not only status reading and control of the drone sensors and functions, but also control and feedback from any custom payloads. During the finals testing, a total of four such wireless nodes were utilized to collect eDNA samples at 1.4 km, beyond the range of the stock DJI remote, and maintaining connection throughout. At the base station, one module on top of a 7 m rollable mast (Rolatube System 75 single tube mast) enabled the base-station laptop to connect to the mesh network over WiFi for feedback and control. A second node was located on the communication raft (yellow dot in Figure 11), which was placed around 300 m from the base camp, thus providing an intermediate node for the UAVs. The last nodes were located on each of the two DJI M300 UAVs. One drone carried out the sampling, while the other acted as a relay drone, positioned between the communication raft and the the sampling drone (the same configuration as in Figure 6). The nodes on the UAVs enable both connection of the onboard computer on the UAV with the ground station and extension of the mesh network. This setup was only used for the furthest three surface eDNA samples, including the one at 1.4 km, demonstrating access across the full 100 ha area.

VIII. AUTONOMOUS SURFACE eDNA COLLECTION

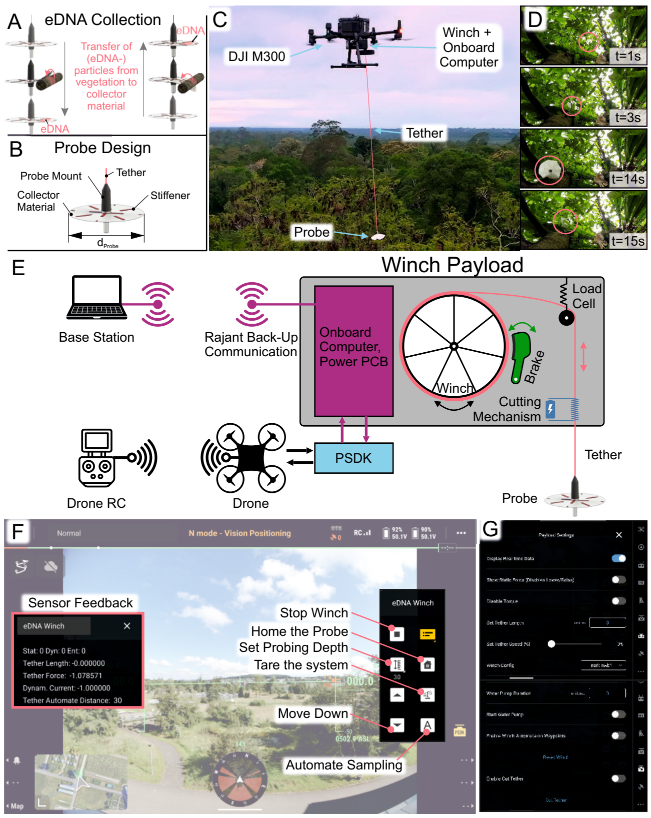

FIGURE 7. Surface eDNA collection mechanism (A-E), teleoperation interface (F,G).

In [31] the eProbe is first described, a payload system used for collecting surface eDNA using a swab which is lowered and raised into the vegetation, as used by the ETH BiodivX team in the XPRIZE Rainforest semi-finals in Singapore. For the XPRIZE Rainforest finals, an upgraded version of the system is used. Mechanically, this has been simplified from two separate compartments, one on top of the drone housing the communication and onboard computer, and one on the bottom containing the winch and electronics, to a single payload which attaches at the bottom and contains all components (Figure 7E). A winch allows lowering of the probe (or pump for water eDNA collection), while a load cell (in black) measures the force on the tether and checks for entanglements or slack in the wire. A hot-wire cutting mechanism (in dark blue) ensures safety in case of terminal entanglements, and LEDs on the box indicate the status of the payload. A brake (in green) allows for locking of the winch to exert more force by moving the drone. Finally, an onboard computer controls, powers, and interfaces all the electronics with a custom PCB. The onboard computer is also directly connected to the Rajant backup communication node on the drone. The payload is mounted via a rail, which also allows mounting of an additional DJI payload, such as a camera. For enhanced usability, the winch payload system utilizes the DJI Payload SDK (PSDK, light blue) interface provided by DJI for payload development [44]. This allows a single USB-C connection from the drone to power the payload, provide access and control from and to the drone, and to forward communication between the onboard computer and the drone RC. Once the payload is plugged in, a custom widget on the default DJI piloting app appears (Figure 7A), allowing full control of the payload. This includes setting the probing depth, moving the probe up and down manually or autonomously, stopping the winch, or taring the load cell. Simple status feedback, such as the length of the tether and force on the winch, is also shown on the screen. Expanded options for configuring settings (such as speed or cutting the tether) are available in a separate menu (Figure 7B). For more comprehensive logging and debugging, a separate SSH connection to the onboard computer can be made and the payload controlled and feedback monitored through the command-line and the base station laptop using the Rajant backup communication network Section VII. This also allows full control of both the payload and drone when the drone is out-of-range of the standard RC.

The points sampled are shown as red dots in Figure 11. A risk-averse sampling strategy was chosen for the competition. With the exception of the three eDNA samples taken at the furthest edge of the area, most of the surface eDNA samples were taken in the lower third of the competition area, within the standard remote range to ensure safety and stable communication. For the same reason, fully autonomous sampling was also performed at these sites. Each cluster of points in the lower third (with the exception of the top left and the middle top, where there were communication issues) is a three by three grid of sub-sampling points, spaced 15 m apart. Similar to the photogrammetry mapping missions, these points were defined beforehand using the UgCS software. Once a new probe is attached to the winch, the drone flies to the first point in the cluster, lowers the probe, then continues to the next point. Once all points in the cluster grid are sampled, the drone returns to exchange the probe.

For full coverage of the competition area, three points were sampled at the far end of the competition area, in a range of up to 1.4 km from the base station. The autonomous missions were planned using the same UgCS mission planning software also used for the mapping missions. Utilizing the RGB orthomosaic, clusters of

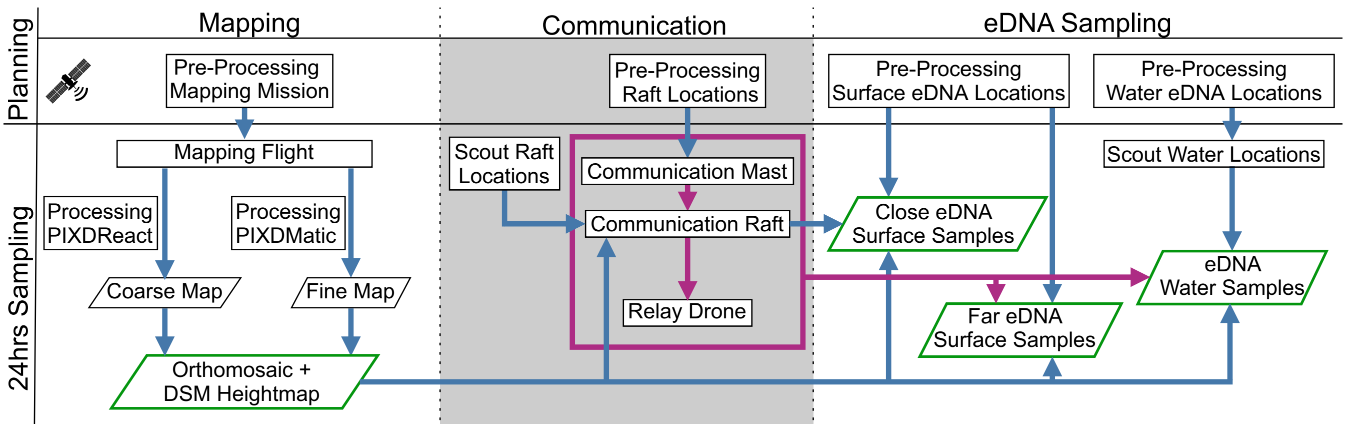

FIGURE 8. eDNA sampling workflows, including autonomous eDNA sampling. Initial satellite-based pre-processing provides potential locations for raft and sampling locations. The two maps are then also used for sampling. The communication network provides connection throughout the competition area.

promising sites are chosen, and the DSM is used to determine the waypoint height. The DSM is loaded into the mission planning software as an elevation map, and thus used for all future planning. Sampling waypoints were set 5-10 meters above the canopy, ensuring operational safety, but also reducing sampling time when lowering the probe and ensuring sufficient sampling depth; with 40 m sampling depth, the forest floor was reached several times. A terrain-adaptive flight path was chosen, so that the drone maintains the same safety distance to the top of the tree canopy, despite undulating terrain. Using the communication connection described in Section VII, the onboard computer which is interfaced with both the custom winch payload and the drone, can provide feedback about the sampling state to the ground station laptop at basecamp and receive commands. Using the DJI Payload-SDK interface, this also allows control and feedback directly from the flight controller, including commanding the drone to return-to-home in case of emergency. For enhanced safety, these samples were taken under supervised autonomy, where the drone flew to the location autonomously, but every lowering of the probe was remotely authorized, however, the system can already be set to carry this out fully autonomously. Once activated, the safety protocols and anti-entanglement algorithm from [31] ensure safety while autonomously lowering and raising the probe with the configured settings. The entire process was commanded and supervised through the back-up communication link described in Section VII, and was far beyond the stock RC range.

To ensure the safety of the drone and the environment, several layers of redundant safety procedures were employed. First, for all samples a communication link was maintained so that feedback could be monitored and commands could be sent to the payload, either through the standard default drone RC, or through the back-up communication link. This includes cutting the tether and return-to-home command for the drone in case of emergency. For the lowering and raising of the probe, an improved algorithm similar to [31] was used to avoid entanglements. If an entanglement is detected, the user is notified with a warning message. The user can then choose to engage a manual brake, which locks the winch spool, and then proceed to raise the drone, which will exert more force to free the probe. The load cell on the winch continues to provide force measurements and can indicate the force on the probe. If this is unsuccessful to disentangle the probe, a hot-wire cutting mechanism can sever the tether and ensure safety of the drone, at the expense of losing a probe and leaving it in the environment. While this was also incorporated into the fully autonomous workflow, it was not enabled for the competition due to the penalty of leaving objects in the environment, and the availability of a continuous communication link. The cutting mechanism itself was not needed, as all ten surface samples were successfully collected without any unresolvable entanglements.

IX. WATER eDNA COLLECTION

Water eDNA can be collected with the same winch payload mechanism described in Section VIII, simply swapping the probe with the custom developed water pump (Figure 9B). First, the drone flies autonomously to the waypoint of water sources detected from close-up images. The H20 camera can also tilt down, providing visual feedback to properly align the pump with the water body. The pump has a separate power source and microcontroller, with a WiFi module that connects to the onboard computer on the drone. This enables control, configuration, and feedback from the pump in the same interface on the drone RC. Even with a downward-facing camera and manual piloting, the distance to the water surface is difficult to estimate, so the pump was set to automatically engage once in the water. For this, the

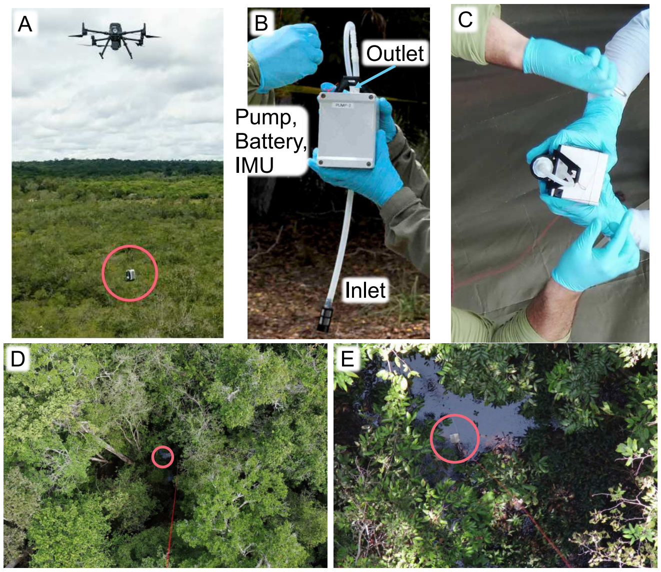

FIGURE 9. Water eDNA collection: A) pump suspended beneath the drone during flight to the selected sampling site, B), C), the pump being disconnected from the tether after sampling D), E), normal and zoomed views of the pump sampling water.

center of gravity of the pump is adjusted so that the pump tilts once it is in the water; an embedded IMU detects this tilt and starts the pump. Simultaneously, the winch lowering is also stopped. The pump filters water through a mesh that retains the eDNA. Once the sampling time has elapsed, the pump stops pumping, and the winch raises the pump. A video of the water sampling is available in the supplementary materials.

A major challenge for water sampling is locating water streams, as they are often concealed beneath dense canopy vegetation. While the rainforest is usually very wet, the drought in the Amazon resulted in lower water levels and fewer water bodies than usual. Temporarily flooded areas and puddles are also suited for water sampling, assuming they are accessible to the pump, requiring a gap in the canopy (at least 5x5 meters) that allows the pump to be safely lowered from the drone. Since large water bodies visible in satellite RGB images were not available in the competition area, regions with a high likelihood of containing water were identified using satellite-based spectral indices (see Figure 3). Those regions were further examined using high-resolution drone RGB orthomosaic maps, and through close-up images from the DJI Mavic 3 Pro and the DJI M300 with the H20. This approach confirmed the presence of accessible water bodies in the southwest and northeast corners of the competition field (see Figure 11).

A total of four water eDNA samples, each approximately 10 liters, were collected (blue dots in Figure 11) from the southwest corner of the competition area. For safety reasons, the water source in the northeast corner was not sampled, as it was beyond the operational range of the RC. While this source could have been accessed using the same autonomous system with backup communication employed for surface eDNA sampling, the decision was made not to proceed. This was due to the limited clearance in the vegetation through which the pump would have needed to be lowered, as well as the absence of a self-disentanglement mechanism in the pump.

X. RAFT

Building on the concept of a walkable inflatable raft that rests atop the canopy layer, our solution takes this idea further by developing an unmanned version. Our design of a drone-deployable canopy raft, depicted in Figure 10, leverages the canopy's capacity to support loads of up to 1.7 kg/m^2 [45] and the mobility of aerial robots to precisely and securely deploy sensors onto the canopy from above. The raft is constructed from lightweight materials engineered to distribute weight evenly across the treetops, minimizing environmental impact on the delicate ecosystem. Once deployed, it serves as a stable platform for deploying instruments for various observations. During the competition, we deployed three sensing rafts in the afternoon, which collected data overnight. The rafts were retrieved at dawn the following morning. Additionally, a communication raft was deployed to establish the mesh network.

A. STRUCTURE

To deliver the rafts' payload to the tree tops, a retrievable hexagonal platform of 2 m diameter was designed to support the load of both the structure and payload on the upper canopy layer (see bottom structure in Figure 10A). The raft has been sized to fit the maximum payload of the carrying quadcopter, a DJI M300, of 2.7 kg. Based on the mentioned load capacity of canopies, a minimum contact area of 1.6 m^2 is required to support the maximum payload. For manufacturing convenience, an area of 2.6 m^2 was chosen, including a safety factor of 1.6. The beams are made out of 8 mm carbon rods, center pieces printed in carbon fiber-reinforced high-temperature nylon, and supporting netting is made of polyethylene wires to evenly distribute pressure across the canopy.

For deployment and retrieval, a triangle structure is connected to the top of the payload (Figure 10B and C). At its base is a passive hook release system for deployment. A wide triangular sail made of polyethylene netting aids in retrieving the raft using a triple hook connected to the quadcopter via a 3 m wire. When lifted, the netted area folds upwards under the raft's weight, ensuring the load remains vertically aligned beneath the drone, even if the hook attaches off-center.

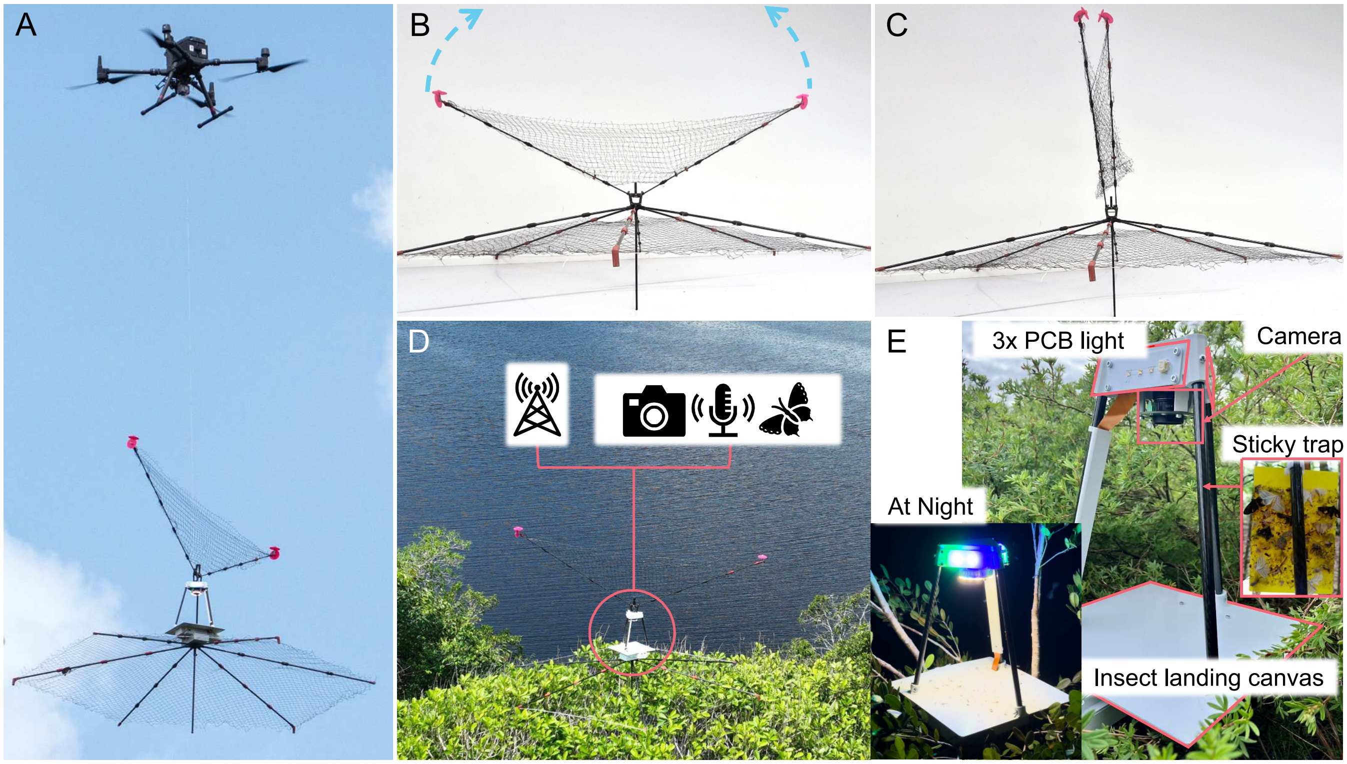

FIGURE 10. A)Field deployment of the raft using a passive hook tethered to a DJI M300 drone, equipped with the PTS4 camera-payload drop system. The supporting lower structure is netted to prevent the structure from sinking into the foliage, with a vertical rod at the center to prevent slipping sideways. B) and C) Passive folding mechanism on the upper part of the raft provides a large netted area that can be easily hooked during the retrieval. D) Raft deployed on a tree. The payload is fixed between the lower structure and the retrieval net. The modular design allows for different missions by attachment of different payloads: biodiversity sensing payload or communication payload. E) Overview of the biodiversity sensing payload and its main components.

For both deployment and retrieval, the PTS4 payload release mechanism with a downward-facing camera was used to allow visualization of the raft and as an emergency release. This mechanism, including the carrying wires and frame, adds up to a weight of less than 160 g.

The connection to the payload is made with a top-down universal M5 bolt-nut configuration, ensuring a modular, fast-to-set-up design with easily exchangeable payloads (Figure 10D). We developed a payload for communication by integrating a Rajant module elevated by a 1 meter carbon beam Figure 6, and a biodiversity sensing payload, described hereafter.

The top and bottom structures are robust for rugged handling during the competition and add up to 610 g in total, and they quickly assemble without additional tools. This design can be further reduced to 500 g or less if more carefully optimized. Disassembled, the structures fit in a regular 120 cm poster tube for easy transportation and protection.

B. RAFT DEPLOYMENT

The deployment of the canopy raft takes place in 3 main steps.

During **pre-deployment**, the DJI Mavic 3 Pro manually scouts for a suitable location. For the raft, a flat, dense tree top is ideal for the safest deployment, while angled deployments of up to 30° have also been found to be stable. Once a suitable location is identified, a descent onto the landing region is performed to verify connection reliability with the RC. The GPS coordinates of the candidate landing spot are then saved for the next step.

This scouting can be automated if a 3D scan of the target area is available. Flat sections can then be identified with available Python scripts using a sliding window function estimating the flatness of the upper percentage of the pointcloud [1].

Deployment itself is done by taking off with the carrying drone, connecting the passive hook to the raft, and flying (optionally autonomously) to the preplanned GPS waypoint. Upon arrival, the drone is teleoperated to perform final alignment with the target landing area, and to gradually descend until the raft settles on the canopy. At this point, the cable connecting the drone to

[1] https://github.com/georg-strunck/LOcalize_Flat_Topped_Trees_Yonder

the raft becomes slack, allowing the hook to passively release under its own weight.

For **retrieval** a triple fishing hook is attached to the drone, which then flies to the canopy raft location. Once there, the drone is teleoperated to lower in a step-wise fashion, moving laterally towards the catching sail at each step. Pink high visibility markers have been added to the design, allowing better judgment (and possible future automation) of the orientation and location of the raft with respect to the drone, as well as depth. Once connected, the raft is gently pulled up vertically to a safe traveling altitude and then returned to the base station.

Video of the raft deployment and retrieval is available in the supplementary materials.

C. SENSING PAYLOAD

The sensing payload is designed as a low-cost, lightweight, and portable device capable of automatically capturing images of insects, recording animal sounds, and collecting insect specimens (Figure 10E). Weighing only 1.3 kg, including two Li-ion batteries with a combined capacity of 10000 mAh, enabling up to 12 hours of continuous operation.

The mechanical structure of the insect light trap consists of three carbon tubes and an optimized 3D-printed case with integrated electronics. The insect light trap also features a geofencing capability, allowing users to set up a geofence with four coordinates, enabling the trap to automatically start operating within the desired geolocation. The insect light trap features a custom PCB that connects electronic subsystems, which is encapsulated inside the electronics box and has an integrated battery monitoring system that safeguards against battery drainage and data loss.

The insect light trap employs three insect light PCBs made of aluminum for heat dissipation. Each PCB contains blue, green, and UV power LEDs, chosen for their specific wavelengths to attract and confuse insects, causing them to land on the insect landing canvas. The insect landing canvas is illuminated by a custom PCB ring spotlight with 10 power LEDs, and insects are photographed by a 12 MP HQ camera, providing high-resolution images for the insect detection algorithm. Images are automatically captured every 10 seconds by default and saved with time, date, and GPS position on an accessible SD card.

In addition to visual data, the sensing payload also records animal sounds using an integrated AudioMoth, sampling at 384,000 samples per second and capturing frequencies up to 192 kHz. All data is stored on accessible SD cards.

Additionally, during operation, insect specimens are collected on yellow sticky traps mounted on the carbon tubes with a mechanical snap mechanism for easy attachment and removal (Figure 10E). Some of the insects attracted by the lights of the camera trap are thus collected in the sticky traps for barcoding analysis.

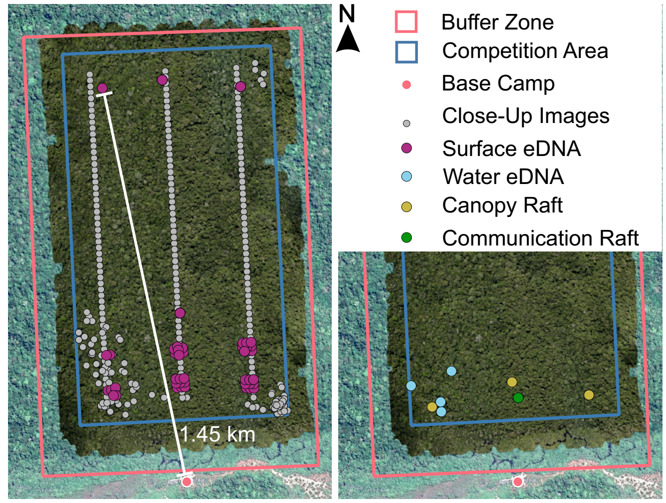

FIGURE 11. Overview of the sample area with each of the different types of samples collected.

XI. RESULTS

An overview of the competition area (dark blue rectangle) along with each of the samples collected can be seen in Figure 11. Gray dots indicate close-up images, captured both manually and autonomously for species identification or for scouting for water locations such as in the top right inset image (see Section VI). Water eDNA sampling is indicated by the light blue dots and was conducted in the southwest corner, within manual RC range (see Section IX). The purple dots indicate surface samples, with the bottom 2 by 3 rows of samples consisting each of a cluster of nine separate probe lowerings in a grid (see Section VIII). The three samples at the far end were conducted with the mesh communication network described in Section VII. The tan dots indicate canopy raft locations (Section X), and the green dot the communication raft.

Total Drone Flights	54
Distance Flown	108.85 km
Total Flight Time	17h 35min
Water Samples Collected	42 L
Length Swabbed	1.38 km
Maximum Depth Swabbed	40 m
eDNA Samples Collected	14
Rafts Deployed	4
Sticky Traps Collected	9
Audio Segments Recorded	3,846

TABLE 2. Summary statistics of collected samples, data, and drone flights.

SampleID	Impacts	Entanglements	Duration
S_002	84	1	00:15:43
S_004	85	0	00:13:41
S_005	60	6	00:09:58
S_006	95	9	00:16:01
S_007	87	2	00:15:34
S_008	57	1	00:10:32
S_009	56	4	00:10:50
S_010	47	1	00:10:55
S_011	64	4	00:12:28
S_012	73	6	00:10:55
Total	**708**	**34**	**02:06:36**

TABLE 3. Surface eDNA statistics per probe. Duration is in hh:mm:ss.

Table 2 shows some high-level statistics regarding the number and type of samples collected. In total, the four drones performed 54 flights, covering 108.85 km in around 17 hours. Of this time, 12 hours and 32 min were spent on tasked flights, collecting samples or placing and collecting rafts, see also Figure 13. Three sensing and one communication raft were deployed, 42 L of water filtered for eDNA, 9 sticky traps were collected, and the audio recorders delivered close to 4000 audio segments. For surface eDNA collection, this meant a cumulative 1.38 km swabbed, with depths of up to 40 m.

Statistics for each surface sample probe can be seen in Table 3, including the number of probe impacts and entanglements. The number of impacts and entanglements provides useful estimate of how frequently the probe interacts with vegetation, and thus how much potential surface eDNA is collected. An impact is recorded when the load cell detects a force below a predefined threshold, indicating that the probe has made contact while descending. An entanglement is registered when the load cell measures a force exceeding the threshold during ascent, which triggers the system's autonomous disentanglement protocol (refer to [31] for details). During the competition, no probes were lost to permanent entanglement in the vegetation.

While a comprehensive analysis of the biodiversity insights generated from the robot-collected data is beyond the scope of this article, Figure 12 gives an overview of the different species identified by the different methods. The beta diversity (Dice-Sørensen) can be seen in Figure 12A. The Dice-Sørensen Index equals twice the number of species common to both sites X and Y divided by the sum of the number of species in each site. If two communities are similar, the index is close to 1. A comparison between two samples with a beta diversity value of 1 means that they are identical communities. Conversely, a value of 0 indicates a complete replacement between two communities with no shared species. Figure 12A shows that all solutions detect very different species, except for a small overlap between the sticky traps barcoding and light camera traps, since both these methods focused on the same taxon group, insects, and were even deployed on the same instruments (rafts, Figure 10).

The total operational taxonomic unit (OTU) richness for the three markers used for the eDNA analysis can be seen per sample in Figure 12B. A W prefix indicates a water sample, and S denotes a surface sample. The largest richness was detected for water sample W_004 and surface sample S_011.

Figure 12C showcases a species of bird and bat detected from the bioacoustic recordings. Specimens collected from the sticky trap on the raft can be seen in Figure 12D. Figure 12E has segmented sample insect captures from the camera trap on the raft, and Figure 12F showcases two species of trees identified through drone remote sensing.

The percentage of the total flight time dedicated to each task is in Figure 13. Surface and water eDNA surveys, took over 50% of the total flight time. The deployment and retrieval of the rafts took another 27% of the time, considering two aborted deployment attempts due to poor connectivity with the remote controller and the time required to scout for optimal deployment locations. The collection of close-up and mapping photos accounted for the remaining 23% of the time.

XII. DISCUSSION

A drone-based survey strategy enabled the collection of biodiversity data and samples within a 100-hectare rainforest area in just 24 hours. As illustrated in Figure 12A, most of the detections of each sampling method are unique, demonstrating the complementary nature of these approaches. In our previous work on surface eDNA collection using the probe in the Singaporean rainforest [31], we demonstrated that taxa detection is positively correlated with the probe's penetration depth in the canopy. Collectively, these results demonstrate the importance of integrating multiple survey methods across different forest layers to achieve a thorough biodiversity assessment.

A. MODULARITY

Despite the importance of collecting diverse types of data with correspondingly differing sampling methods, the logistics and effort should still be minimized. This is especially true when considering the transport, powering, charging, and maintenance of different robotic systems. For robustness through simplicity, we employed the "Swiss-Army Knife" approach to our robots, with a single drone platform that can transport multiple survey tools. This workhorse was the DJI M300, which could mount RGB camera payloads for mapping, a zoom camera for close-up images or scouting for good raft locations

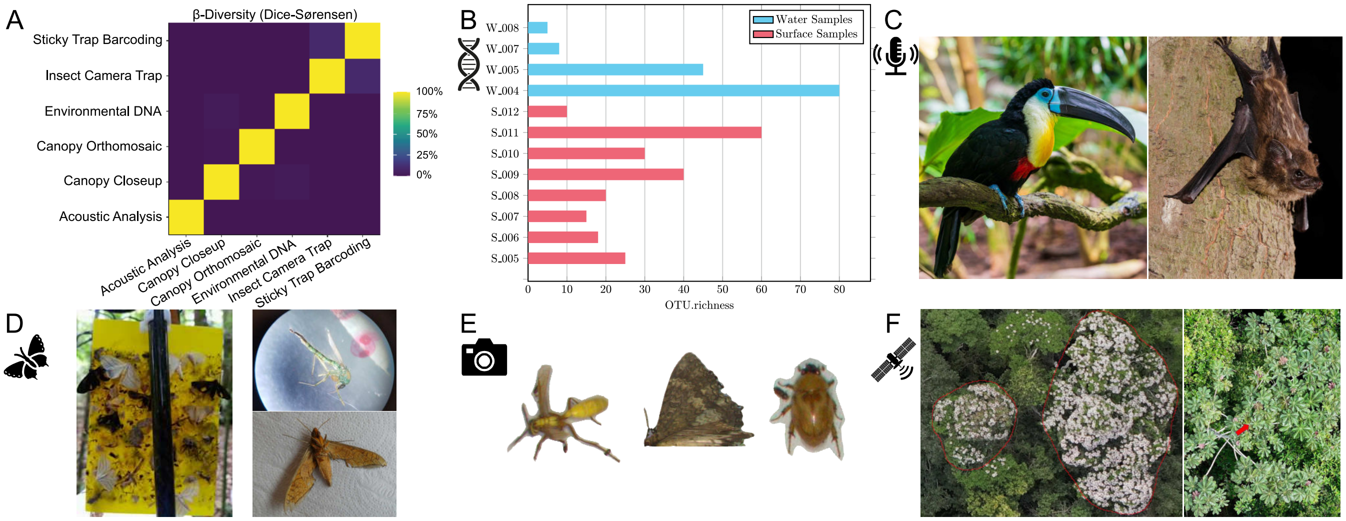

FIGURE 12. **Overview of species detections by method. A) Heat map showing the beta diversity between the detection methods used in our solution, darker colors show little to no overlap, while lighter (yellow) colors show a larger overlap. B) Total OTU richness combined for all analyzed markers per eDNA sample. The water sample W_004 showed the highest richness, while in the sample W_008 we detected the lowest richness of five OTUs. C) Two sample species detected from the bioacoustic recordings, a channel-billed toucan (*Ramphastos vitellinus*) and the Lesser Sac-winged Bat (*Saccopteryx leptura*). D) The sticky trap (left) and two sample specimens, a non-biting midge (Family *Chironomidae*) (top), and a streaked sphinx (*Protambulyx strigilis*) (bottom). E) Sample insects from the camera trap on the raft (left to right): *Apoica flavissima*, Scops Witch Moth (*Feigeria scops*), and *Cyclocephala lunulata*. F) Two tree speices identified through drone remote sensing, *Anacardium spruceanum* (left), and *Cecropia distachya* (right).**

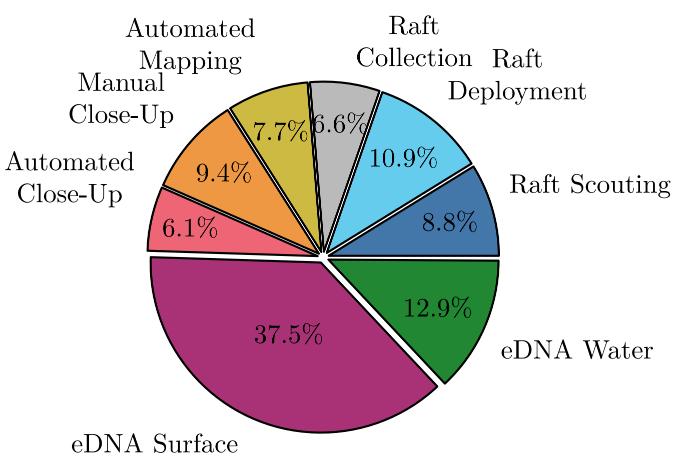

FIGURE 13. **UAV flight time breakdown per task. (Total tasked flight time: 12hours, 32m)**

or water sources, a winchbox and probe for surface eDNA collection, or a water pump for water eDNA, as well as a mechanism for deploying and retrieving the canopy rafts. Enabling these diverse tasks with a single platform not only reduces logistical overhead, but also financial investment, since only a single robot and corresponding batteries are needed. For the competition two DJI M300s and two DJI Mavics were used, however this was mainly for parallelization and redundancy due to the time and robustness constraints imposed by the competition. When not all sampling methods have to be deployed and collected within 24 hours, a single drone with swappable payloads is sufficient to collect these data.

B. TECHNOLOGY READINESS LEVEL

Due to the tight time constraints of collecting all samples within 24 hours, and necessary reliability of the solutions to cover the 100 ha and work in challenging environments and climate conditions, the deployed platforms require a high TRL. Fundamentally, this requires simple systems which are robust, user-friendly, and efficient at collecting data. For these reasons, we focused on developing reliable sampling payloads, mission planning, and system integration, while using an off-the-shelf drone. An off-the-shelf drone offers industry grade flight performance and reliability, with both hardware and software integration available for custom payloads. This focus has resulted in payloads such as the eProbe winchbox, which has proved highly robust, reliable, and easy-to-use, even in other sampling campaigns outside of the competition. Through focus on customized payloads and mission planning, we minimized development time and ensured smooth operation in the field. However, this approach also fundamentally limits the functions that can be realized. A major limitation is the closed hardware and software ecosystem of the DJI drone, with certain sensors and functions available through the developer SDK only at the drone manufacturer's discretion. A custom-build platform on the other hand, can be fully accessed and customized. This also limits potential applications, for instance, flying beneath the canopy.

C. AUTONOMY VS TELEOPERATION

Both autonomous and teleoperated solutions were deployed by our team for this competition (Figure 2).

Raft deployment and collection, and close-up images with the DJI Mavic 3 were teleoperated. Basic flight stabilization and obstacle avoidance from the drone were utilized, but piloting, selection of the sampling location and data collection were under direct control of the operator. Next are partially autonomous samplings, for instance, surface and water eDNA sampling. Once the sampling is initiated, no further user input is required. The flight to the sampling location can either be manual or conducted as a waypoint mission. The highest level of autonomy was for the mapping and programmed close-up image collection. These were fully autonomous once the flight path was generated, and also did not require a communication link to the pilot. This demonstrates a key benefit of autonomy: range. Since teleoperated drones require a constant communication link with the pilot, this greatly reduces the operational range of the drone, especially under challenging conditions such as in the rainforest. While methods of maintaining a connection can extend the range, such as in our case up to 1.4 km, this is also correlated with greatly increased effort. In our case, this required a mesh network and communication nodes mounted on a mast, a communication raft, and a relay drone. An autonomous drone does not require any of this, and can thus fly to the limits of its batteries, but must also be sufficiently autonomous to respond safely in any eventuality. Increased automation also correlates with reduced pilot effort and increased usability. However, removing the human from the loop completely is also not desired. Not only is it technically challenging, since it requires all eventualities to be covered from a safety perspective, but human input is essential for high-level tasks such as sampling site selection. For certain applications, higher autonomy can actually increase the total time needed per sample area. Human-supervised semi-autonomous systems can actually be faster since the human-in-the-loop can speed up certain processes depending on environmental factors, for instance, increasing flight speed in the absence of obstacles. Increased safety requirements and checks result in slower systems, and autonomous systems require additional safety checks. Partial automation of repetitive and high-effort tasks while keeping the pilot in the control loop presents a good compromise between usability and automation.

D. VEGETATION DENSITY AS AN ASSET

Usually in robotics, dense and cluttered vegetation is treated as an obstacle that should be circumvented or avoided. However, it is also possible to leverage the density and unstructured nature of vegetation as an asset. For example, collecting eDNA with the eProbe requires direct contact between the collector material and the environment, with the amount of eDNA collected positively correlating with the number, duration, and force of these contacts [31]. Since the eProbe descends passively through the canopy without additional directional actuators, it does not actively target specific surfaces to contact, but instead it relies on chance and sufficient repetitions to collect eDNA. In this case, dense vegetation is beneficial since there is an increased likelihood of contacts. Since the design of the eProbe minimizes the risk of entanglements, denser jumbles of branches and leaves transform from risky regions to be avoided, to areas that should be sampled due to the higher likelihood of contact. Similarly, for canopy rafts, denser regions of the canopy represent areas that can safely sustain higher loads and are preferred and sought out over sparser areas when placing the raft.

E. LIMITATIONS AND FUTURE WORK

The showcased systems demonstrated successful assessment of biodiversity within the competition framework, however, there is still room for improvement. While the competition covered 100 ha in 24 hours, comprehensive biodiversity assessments will require scaling in both temporal and spatial dimensions.

Extending the operational time of the canopy rafts would require the integration of solar charging systems and the capability to stream data via a mesh network or low-bandwidth satellite up-link. More frequent eDNA sampling could benefit from commercially available drone-in-a-box solutions; however, this would necessitate further automation of the eDNA analysis workflow, including collector preparation, eDNA extraction, and genetic analysis. Consequently, intermittent field sampling remains the most feasible approach in the near term.

Scaling surveys beyond the 100-hectare area covered during the competition will require a strategic integration of in-situ sampling with remote sensing data [46]–[48]. Specifically, in-situ observations can be used to calibrate and validate species distribution models and community-level diversity metrics derived from environmental covariates such as canopy height, structure, and heterogeneity extracted from remote sensing.

Another important direction for improvement is increasing the efficiency of the survey through a more strategic and informed planning. During the competition, maps were utilized to inform sampling locations, including identifying accessible water sources and defining waypoints for autonomous surface eDNA collection. Future missions could take this further by using maps to compute variables that influence eDNA distribution and species presence to derive an “information index.” Sampling locations could then be selected to maximize expected information gain, thereby reducing sampling effort while enhancing ecological insight. Ideally, such analysis and optimization would be performed onboard, leveraging AI-enabled aerial robots in combination with ecological priors and contextual knowledge.

The use of drones in canopy research not only enables accessibility to complex ecosystems, but also improves the spatial resolution of collected data, thanks to the inherent wide coverage that drones provide. Beyond data collection, drones facilitate faster analysis by enabling the rapid collection and transport of samples to research stations. These advancements have the potential to reduce human impact on fragile habitats and pave the way for new frontiers in biodiversity monitoring and ecological research. However, despite cost reductions over the years, the large up-front acquisition cost, high-turnover, and rapid obsolescence of drones represent a relatively high barrier to entry. Considering that most biodiverse regions in the world are in the global south, directing future work towards reducing the necessary equipment and material costs would yield more inclusive and equitable solutions for biodiversity monitoring.

XIII. CONCLUSION

In this work, we have described team ETH BiodivX's robotic solutions for the XPRIZE Rainforest Final competition, our contribution to address the pressing challenge of rapidly assessing biodiversity in some of the most challenging environments. Our approach consisted of integrated remote and in-situ sampling enabled by aerial robots. A single drone platform enables most of the tasks through modular and switchable payloads. First, we map the entire 100 ha and generate an orthomosaic and DSM within one and a half hours. This initial data is then used for waypoints to autonomously collect surface eDNA with the eProbe winch system. The same winch system can also collect water eDNA by attaching a custom water sampling pump. For longer-term data collection and diversified data sources, canopy rafts with insect traps are manually deployed within the competition area. The canopy rafts are equipped with bioacoustic recorders, a camera trap that attracts and photographs insects, and stick traps for collecting physical samples for barcoding. A separate communication raft is part of a mesh network spanning from a mast at the base-station to a relay drone, and permit a stable communication connection throughout the 100 ha to safely monitor and trigger surface eDNA sampling at the furthest points of the competition area, at distances of 1.4 km. Through the developed solutions, our team was able to win the bonus prize in the XPRIZE Rainforest Competition, taking the first step towards highly usable and automated robotic solutions for assessing biodiversity in rainforest canopies at scale.

ACKNOWLEDGMENT

The authors extend their heartfelt gratitude to Zoo Zürich for their invaluable support in developing eDNA sampling solutions within the Masoala Rainforest Halle. Special thanks go to Luca Desiderato and Veronica Condello for providing exceptional media materials, Gabriela Devaud and Sofia Costa from SwissNex Brazil, and Duno Gerber, for their invaluable support to the team in Brazil. The authors also thank the entire ETH BiodivX team from the XPRIZE Rainforest competition for their collaborative spirit and constructive feedback, which greatly contributed to advancing our solutions for improving biodiversity discovery and rainforest monitoring.

REFERENCES

[1] S. L. Lewis, D. P. Edwards, and D. Galbraith, "Increasing human dominance of tropical forests," *Science*, vol. 349, no. 6250, pp. 827–832, 2015. [Online]. Available: http://science.sciencemag.org/content/349/6250/827

[2] N. E. Stork, J. Balston, G. D. Farquhar, P. J. Franks, J. A. M. Holtum, and M. J. Liddell, "Tropical rainforest canopies and climate change," *Austral Ecology*, vol. 32, no. 1, pp. 105–112, 2007. [Online]. Available: https://onlinelibrary.wiley.com/doi/10.1111/j.1442-9993.2007.01741.x

[3] R. Pillay, M. Venter, J. Aragon-Osejo, P. González-del-Pliego, A. J. Hansen, J. E. Watson, and O. Venter, "Tropical forests are home to over half of the world's vertebrate species," *Frontiers in Ecology and the Environment*, vol. 20, no. 1, pp. 10–15, 2 2022. [Online]. Available: https://onlinelibrary.wiley.com/doi/full/10.1002/fee.2420

[4] J. Liu, F. Slik, S. Zheng, and D. B. Lindenmayer, "Undescribed species have higher extinction risk than known species," *Conservation Letters*, vol. 15, no. 1, p. e12876, 2022.

[5] M. Hedblom, R. J. D. Siddall *et al.*, "Robotics and autonomous systems for environmental sustainability: Monitoring terrestrial biodiversity," *UK-RAS white papers*, 2023.

[6] C. J. Marsh, E. C. Turner, B. W. Blonder, B. Bongalov, S. Both, R. S. Cruz, D. M. O. Elias, D. Hemprich-Bennett, P. Jotan, V. Kemp, U. H. Kritzler, S. Milne, D. T. Milodowski, S. L. Mitchell, M. M. Pillco, M. H. Nunes, T. Riutta, S. J. B. Robinson, E. M. Slade, H. Bernard, D. F. R. P. Burslem, A. Y. C. Chung, E. L. Clare, D. A. Coomes, Z. G. Davies, D. P. Edwards, D. Johnson, P. Kratina, Y. Malhi, N. Majalap, R. Nilus, N. J. Ostle, S. J. Rossiter, M. J. Struebig, J. A. Tobias, M. Williams, R. M. Ewers, O. T. Lewis, G. Reynolds, Y. A. Teh, and A. Hector, "Tropical forest clearance impacts biodiversity and function, whereas logging changes structure," *Science*, vol. 387, no. 6730, pp. 171–175, 1 2025. [Online]. Available: https://www.science.org/doi/10.1126/science.adf9856

[7] M. G. Barker and M. A. Pinard, "Forest canopy research: sampling problems, and some solutions," *Plant Ecology*, vol. 153, pp. 23–38, 2001.

[8] A. Nakamura, R. L. Kitching, M. Cao, T. J. Creedy, T. M. Fayle, M. Freiberg, C. Hewitt, T. Itioka, L. P. Koh, K. Ma, Y. Malhi, A. Mitchell, V. Novotny, C. M. Ozanne, L. Song, H. Wang, and L. A. Ashton, "Forests and Their Canopies: Achievements and Horizons in Canopy Science," *Trends in Ecology & Evolution*, vol. 32, no. 6, pp. 438–451, 6 2017. [Online]. Available: https://linkinghub.elsevier.com/retrieve/pii/S0169534717300599

[9] C. H. Cannon, C. Borchetta, D. L. Anderson, G. Arellano, M. Barker, G. Charron, J. M. LaMontagne, J. H. Richards, E. Abercrombie, L. F. Banin, X. Tagle Casapia, X. Chen, P. Degtjarenko, J. E. Dell, D. Durden, J. E. Guevara Andino, R. Hernández-Gutiérrez, A. D. Hirons, C.-S. Kua, H. La Vigne, M. Leponce, J. Y. Lim, M. Lowman, A. J. Marshall, S. T. Michaletz, B. B. Normark, D. S. Penneys, G. F. Schneider, J. S. Strijk, B. B. Tiamiyu, T. L. E. Trammell, Y. L.

Vargas-Rodriguez, S. R. Weintraub-Leff, A. Lussier Desbiens, and M. Spenko, "Extending Our Scientific Reach in Arboreal Ecosystems for Research and Management," *Frontiers in Forests and Global Change*, vol. 4, 11 2021. [Online]. Available: https://www.frontiersin.org/articles/10.3389/ffgc.2021.712165/full

[10] X. Foundation, "XPRIZE Rainforest Competition." [Online]. Available: https://www.xprize.org/prizes/rainforest

[11] M. Leponce, Y. Basset, A. Aristizabal-Botero, N. Baïben, J. Barbut, B. Buyck, P. Butterill, K. Calders, G. Cárdenas, J.-F. Carrias, D. Catchpole, B. D'hont, J. Delabie, J. Drescher, D. Ertz, A. Heughebaert, V. Hofstetter, C. Leroy, F. Melki, J. Michaux, J. C. Neita-Moreno, E. Poirier, R. Rougerie, G. Rouhan, V. Rufray, S. Scheu, J. Schmidl, A. Vanderpoorten, C. Villemant, N. Youdjou, and O. Pascal, "Unveiling the above-ground eukaryotic diversity supported by individual large old trees: the "Life on Trees" integrative protocol," *Frontiers in Forests and Global Change*, vol. 7, p. 1425492, 8 2024. [Online]. Available: https://www.frontiersin.org/articles/10.3389/ffgc.2024.1425492/full

[12] D. A. Bohan, C. Vacher, A. Tamaddoni-Nezhad, A. Raybould, A. J. Dumbrell, and G. Woodward, "Next-Generation Global Biomonitoring: Large-scale, Automated Reconstruction of Ecological Networks," *Trends in Ecology & Evolution*, vol. 32, no. 7, pp. 477–487, 7 2017. [Online]. Available: https://linkinghub.elsevier.com/retrieve/pii/S0169534717300605

[13] R. van Klink, J. K. Sheard, T. T. Høye, T. Roslin, L. A. Do Nascimento, and S. Bauer, "Towards a toolkit for global insect biodiversity monitoring," *Philosophical Transactions of the Royal Society B: Biological Sciences*, vol. 379, no. 1904, 6 2024. [Online]. Available: https://royalsocietypublishing.org/doi/10.1098/rstb.2023.0101

[14] M. Besson, J. Alison, K. Bjerge, T. E. Gorochowski, T. T. Høye, T. Jucker, H. M. R. Mann, and C. F. Clements, "Towards the fully automated monitoring of ecological communities," *Ecology Letters*, vol. 25, no. 12, pp. 2753–2775, 12 2022. [Online]. Available: https://onlinelibrary.wiley.com/doi/10.1111/ele.14123

[15] R. Dial and S. C. Tobin, "Description of arborist methods for forest canopy access and movement," *Selbyana*, vol. 15, no. 2, pp. 24–37, 1994. [Online]. Available: https://www.jstor.org/stable/41760268

[16] L. Picart, P.-M. Forget, C. A. D'Haese, C. Daugeron, S. Beni, R. Bounzel, E. Kergresse, F. Legendre, J. Murienne, and E. Guilbert, "The cafotrop method: An improved rope-climbing method for access and movement in the canopy to study biodiversity," *Ecotropica*, vol. 20, pp. 45–52, 2014. [Online]. Available: https://www.soctropecol.eu

[17] S. J. Wright, A. E. Zanne, D. D. Ackerly, and et al., "Assessing the above-ground biomass of a complex tropical rainforest using a canopy crane," *Functional Ecology*, vol. 24, no. 6, pp. 1332–1344, 2010.

[18] H.-P. Aberlenc, L. Andriamampianina, E. Faure, D. C. Lees, J. Minet, L. Ollivier, C. Rafamantanantsoa, M. Randrianandrasana, and A. Razafindrakotomamonjy, "Le radeau des cimes au parc national de masoala (madagascar). première partie : éléments pour un inventaire des lépidoptères," *Bulletin mensuel de la Société linnéenne de Lyon*, vol. 76, no. 6, pp. 141–154, 2007. [Online]. Available: https://www.persee.fr/doc/inly_0366-1326_2007_num_76_6_13658

[19] L. Zheng and S. Hamaza, "ALBERO: Agile Landing on Branches for Environmental Robotics Operations," *IEEE Robotics and Automation Letters*, pp. 1–8, 2024. [Online]. Available: https://ieeexplore.ieee.org/document/10380767/

[20] S. Sharma, M. Verhoeff, F. Joosen, R. V. Prasad, and S. Hamaza, "A morphing quadrotor-blimp with balloon failure resilience for mobile ecological sensing," *IEEE Robotics and Automation Letters*, 2024.

[21] L. Wang, M. Clayton, and A. G. Rossberg, "Drone audition for bioacoustic monitoring," *Methods in Ecology and Evolution*, vol. 14, no. 12, pp. 3068–3082, 12 2023. [Online]. Available: https://onlinelibrary.wiley.com/doi/full/10.1111/2041-210X.14234

[22] H. Löcken, O. W. Fischer, J. Selz, and M. Boppré, "'Drone-Netting' for Sampling Live Insects," *Journal of Insect Science*, vol. 20, no. 5, pp. 3–4, 9 2020. [Online]. Available: https://dx.doi.org/10.1093/jisesa/ieaa086

[23] G. Charron, T. Robichaud-Courteau, H. La Vigne, S. Weintraub, A. Hill, D. Justice, N. Bélanger, and A. Lussier Desbiens, "The DeLeaves: a UAV device for efficient tree canopy sampling," *Journal of Unmanned Vehicle Systems*, vol. 8, no. 3, pp. 245–264, 9 2020. [Online]. Available: http://www.nrcresearchpress.com/doi/10.1139/juvs-2020-0005

[24] A. K. Schweiger, A. Lussier Desbiens, G. Charron, H. La Vigne, and E. Laliberté, "Foliar sampling with an unmanned aerial system (UAS) reveals spectral and functional trait differences within tree crowns," *Canadian Journal of Forest Research*, vol. 50, no. 10, pp. 966–974, 10 2020. [Online]. Available: https://cdnsciencepub.com/doi/10.1139/cjfr-2019-0452http://www.nrcresearchpress.com/doi/10.1139/cjfr-2019-0452

[25] S. Hamaza, I. Georgilas, M. Fernandez, P. Sanchez, T. Richardson, G. Heredia, and A. Ollero, "Sensor installation and retrieval operations using an unmanned aerial manipulator," *IEEE Robotics and Automation Letters*, vol. 4, no. 3, pp. 2793–2800, 2019.

[26] S. Hamaza, H. Nguyen, and M. Kovac, "Sensor delivery in forests with aerial robots: A new paradigm for environmental monitoring," in *IEEE IROS Workshop on Perception, Planning and Mobility in Forestry Robotics*, 2020.

[27] C. Geckeler and S. Mintchev, "Bistable Helical Origami Gripper for Sensor Placement on Branches," *Advanced Intelligent Systems*, vol. 4, no. 10, p. 2200087, 10 2022. [Online]. Available: https://onlinelibrary.wiley.com/doi/10.1002/aisy.202200087

[28] C. Geckeler, B. A. Pizzani, and S. Mintchev, "Biodegradable Origami Gripper Actuated with Gelatin Hydrogel for Aerial Sensor Attachment to Tree Branches," in *Proceedings - IEEE International Conference on Robotics and Automation*, vol. 2023-May. IEEE, 5 2023, pp. 5324–5330. [Online]. Available: https://ieeexplore.ieee.org/document/10160316/

[29] S. Kirchgeorg, E. Aucone, F. Wenk, and S. Mintchev, "Design, Modeling and Control of AVOCADO: A Multimodal Aerial-Tethered Robot for Tree Canopy Exploration," *IEEE Transactions on Robotics*, pp. 1–14, 2023. [Online]. Available: https://ieeexplore.ieee.org/document/10323196/

[30] E. Aucone, S. Kirchgeorg, A. Valentini, L. Pellissier, K. Deiner, and S. Mintchev, "Drone-assisted collection of environmental DNA from tree branches for biodiversity monitoring," *Science Robotics*, vol. 8, no. 74, p. eadd5762, 1 2023. [Online]. Available: https://www.science.org/doi/10.1126/scirobotics.add5762

[31] S. Kirchgeorg, J. J. M. Chang, Y. C. A. Ip, M. Jucker, C. Geckeler, M. Lüthi, E. van der Loo, E. Mächler, N. D. Franco-Sierra, M. A. G. Herrera, L. Pellissier, K. Deiner, A. Desiderato, and S. Mintchev, "eProbe: Sampling of Environmental DNA within Tree Canopies with Drones," *Environmental Science & Technology*, 9 2024. [Online]. Available: https://pubs.acs.org/doi/10.1021/acs.est.4c05595

[32] M. T. P. Coelho, E. Barreto, T. F. Rangel, J. A. F. Diniz-Filho, R. O. Wüest, W. Bach, A. Skeels, I. R. McFadden, D. W. Roberts, L. Pellissier, N. E. Zimmermann, and C. H. Graham, "The geography of climate and the global patterns of species diversity," *Nature*, vol. 622, no. 7983, pp. 537–544, 10 2023. [Online]. Available: https://www.nature.com/articles/s41586-023-06577-5

[33] J. Müller, O. Mitesser, H. M. Schaefer, S. Seibold, A. Busse, P. Kriegel, D. Rabl, R. Gelis, A. Arteaga, J. Freile, G. A. Leite, T. N. de Melo, J. LeBien, M. Campos-Cerqueira, N. Blüthgen, C. J. Tremlett, D. Böttger, H. Feldhaar, N. Grella, A. Falconí-López, D. A. Donoso, J. Moriniere, and Z. Buřivalová, "Soundscapes and deep learning enable tracking biodiversity recovery in tropical forests," *Nature Communications*, vol. 14, no. 1, p. 6191, 10 2023. [Online]. Available: https://www.nature.com/articles/s41467-023-41693-w

[34] L. A. Ashton, H. S. Barlow, A. Nakamura, and R. L. Kitching, "Diversity in tropical ecosystems: the species

richness and turnover of moths in Malaysian rainforests," *Insect Conservation and Diversity*, vol. 8, no. 2, pp. 132–142, 3 2015. [Online]. Available: https://onlinelibrary.wiley.com/doi/full/10.1111/icad.12090

[35] K. Deiner, E. A. Fronhofer, E. Mächler, J.-C. Walser, and F. Altermatt, "Environmental DNA reveals that rivers are conveyer belts of biodiversity information," *Nature Communications*, vol. 7, no. 1, p. 12544, 8 2016. [Online]. Available: https://www.nature.com/articles/ncomms12544

[36] R. Wang, J. A. Gamon, J. Cavender-Bares, P. A. Townsend, and A. I. Zygielbaum, "The spatial sensitivity of the spectral diversity–biodiversity relationship: an experimental test in a prairie grassland," *Ecological Applications*, vol. 28, no. 2, pp. 541–556, 3 2018. [Online]. Available: https://onlinelibrary.wiley.com/doi/full/10.1002/eap.1669

[37] A. Huete, "A comparison of vegetation indices over a global set of TM images for EOS-MODIS," *Remote Sensing of Environment*, vol. 59, no. 3, pp. 440–451, 3 1997. [Online]. Available: https://linkinghub.elsevier.com/retrieve/pii/S0034425796001125

[38] S. K. McFEETERS, "The use of the Normalized Difference Water Index (NDWI) in the delineation of open water features," *International Journal of Remote Sensing*, vol. 17, no. 7, pp. 1425–1432, 5 1996. [Online]. Available: https://www.tandfonline.com/doi/full/10.1080/01431169608948714

[39] G. P. Asner, M. Palace, M. Keller, R. Pereira, J. N. M. Silva, and J. C. Zweede, "Estimating Canopy Structure in an Amazon Forest from Laser Range Finder and IKONOS Satellite Observations 1," *Biotropica*, vol. 34, no. 4, pp. 483–492, 12 2002. [Online]. Available: https://onlinelibrary.wiley.com/doi/10.1111/j.1744-7429.2002.tb00568.x

[40] R. E. Kennedy, Z. Yang, N. Gorelick, J. Braaten, L. Cavalcante, W. B. Cohen, and S. Healey, "Implementation of the LandTrendr Algorithm on Google Earth Engine," *Remote Sensing*, vol. 10, no. 5, p. 691, 5 2018. [Online]. Available: https://www.mdpi.com/2072-4292/10/5/691

[41] S. Engineering, "UGCS." [Online]. Available: https://www.sphengineering.com/flight-planning/ugcs

[42] Pix4D, "Pix4D." [Online]. Available: https://www.pix4d.com/

[43] Rajant, "Rajant Breadcrumb DX2." [Online]. Available: https://rajant.com/products/breadcrumb-wireless-nodes/dx-series/

[44] DJI, "DJI Payload SDK." [Online]. Available: https://developer.dji.com/payload-sdk/

[45] F. Hallé, D. Cleyet-Marrel, and G. Ebersolt, *Le Radeau des Cimes: L'exploration des canopées forestières*. JC Lattès, April 2000.

[46] J. Cavender-Bares, F. D. Schneider, M. J. Santos, A. Armstrong, A. Carnaval, K. M. Dahlin, L. Fatoyinbo, G. C. Hurtt, D. Schimel, P. A. Townsend, S. L. Ustin, Z. Wang, and A. M. Wilson, "Integrating remote sensing with ecology and evolution to advance biodiversity conservation," *Nature Ecology & Evolution*, vol. 6, no. 5, pp. 506–519, 3 2022. [Online]. Available: https://www.nature.com/articles/s41559-022-01702-5

[47] Y. Li, C. Devenish, M. I. Tosa, M. Luo, D. M. Bell, D. B. Lesmeister, P. Greenfield, M. Pichler, T. Levi, and D. W. Yu, "Combining environmental DNA and remote sensing for efficient, fine-scale mapping of arthropod biodiversity," *Philosophical Transactions of the Royal Society B: Biological Sciences*, vol. 379, no. 1904, 6 2024. [Online]. Available: https://royalsocietypublishing.org/doi/10.1098/rstb.2023.0123

[48] B. Wildermuth, A. Penanhoat, H. Sennhenn-Reulen, D. Matevski, J. Drescher, M. Aubry-Kientz, D. Seidel, and A. Schuldt, "Canopy structure influences arthropod communities within and beyond tree identity effects: Insights from combining LiDAR data, insecticidal fogging and machine learning regression modelling," *Ecological Indicators*, vol. 160, p. 111901, 3 2024. [Online]. Available: https://linkinghub.elsevier.com/retrieve/pii/S1470160X24003583